Hindawi Publishing Corporation
Journal of Nanomaterials
Volume 2010, Article ID 910434, 8 pages
doi:10.1155/2010/910434

Research Article

Uptake and Cytotoxicity of Ce(IV) Doped TiO_2 Nanoparticles in Human Hepatocyte Cell Line L02

Jian Mao,[1] Long Wang,[1,2] Zhiyong Qian,[3] and Mingjing Tu[1]

[1] *College of Material Science and Engineering, Sichuan University, Chengdu, 610064 Sichuan, China*
[2] *Institute of Zhongshan Opto-electronics, Zhongshan Torch Polytechnic, Zhongshan 528436, Guangdong, China*
[3] *State Key Laboratory of Biotherepy, West China Hospital, Sichuan University, Chengdu, 610041 Sichuan, China*

Correspondence should be addressed to Jian Mao, maojianemail@163.com and Zhiyong Qian, anderson-qian@163.com

Received 4 September 2009; Revised 29 November 2009; Accepted 8 March 2010

Academic Editor: Huisheng Peng

Ce(IV) doped anatase TiO_2 nanoparticles (CDTs) were prepared and the underlying mechanism by which CDT nanoparticle enters into cell and its cytotoxicity were investigated in a human hepatocellular line L02 cell. The results showed that CDTs can enter into cytoplasm of L02 cell via endocytosis and nonendocytic ways. Large aggregation of CDTs went into cell by endocytosis and finally formed an endocytic vesicle with membrane boundary. Tiny aggregation of CDTs entered into cell cytoplasm via channels similar to that for lung-blood substance exchange in the alveolar-airway barrier. In addition, tiny aggregation of CDTs was observed in nucleus, and maybe CDTs could pass through the nucleus envelope via the channels provided by nuclear pore complexes (NPCs). Results from MTT assay, fluorescence microscope, and TEM observations showed that the cell viability, cell morphology, cell growth, and cell division periods could not be obviously impaired when cells were exposed to CDTs of different concentration from 30 to 150 μg mL^{-1} without UV irradiation. However, large vacuoles containing CDTs were found in cytoplasm, some structure changes were observed in mitochondria, and smooth envelope around the nucleus was shrank and deformed.

1. Introduction

TiO_2 was previously classified as biologically inert and has been widely used in the cosmetics, pharmaceutical, paint, and paper industries. However, the cytotoxicity of nanosized TiO_2 has caused wide concerns by scientists and engineers in the last decades.

Several studies [1–4] have shown that the cytotoxicity of nanosized TiO_2 was very low or negligible as compared with other nanoparticles. The size was not the effective factor of cytotoxicity [4]. Without UV irradiation, nanosized TiO_2 showed no inflammatory effect or genotoxicity in rats [5] and induced no DNA damages in human cells [6]. In contrast, several studies [7–16] showed the cell cytotoxicity of nano-TiO_2 in vitro. For example, Oberdörster et al. [7] reported that chronic pulmonary inflammation in the rat could be induced by nanosized TiO_2 required the presence of alveolar macrophages. De Virgilio et al. [8] concluded that the presence of TiO_2 nanoparticle in the cell surroundings could lead to cytotoxic effects, which are dependent on the chemical composition, the concentration of the nanoparticles, the exposure time, and the type of treated cell. Rahman et al. [9] reported that in human and rat alveolar macrophages, the level of reactive oxygen species increased after exposure to nanosized TiO_2. The results of Jin et al. [10] showed that the weakly aggregated anatase TiO_2 nanoparticles in solution could induce significant cytotoxicity in L929 cells. In Syrian hamster embryo fibroblasts, ultrafine TiO_2 alone resulted in micronuclei formation and apoptosis [11]. Lai et al. [12] found that TiO_2 micro- and nanoparticles induced cell death on both human astrocytes-like astrocytoma U87 cell and normal human fibroblasts in a concentration-related manner. Nanosized TiO_2 was also reported to affect gene expressions including an apoptosis-related gene [13], especially the following several latest reports supported the genotoxicity of nanosized TiO_2. Wang et al. [14] reported that ultrafine TiO_2 can cause genotoxicity and cytotoxicity in cultured human cells. Reeves et al. [15]

reported that nanosized TiO_2 (0.1–1000 $\mu g\,mL^{-1}$) with UVA irradiation (0.5–2.0 $kJ\,m^{-2}$) could cause a significant cell viability decrease on gold fish skin cell and further increase in DNA damages. Vevers and Jha [16] also reported the similar results; without UVA irradiation, there is little oxidative DNA damage of RTG-2 cells of fish exposure to TiO_2-engineered nanoparticles, whereas a significantly increased level of DNA strand brend breaks was observed in combination with UVA irradiation (3 $kJ\,m^{-2}$).

Anatase TiO_2 has a wide band gap about 3.2 eV, and doping with impurities has been widely used to modify the photocatalysis of TiO_2 by introduction of new states in its electronic structure [17, 18]. In particular, for the unique 4f electron configuration, lanthanide metal ions are ideal dopants to promote a higher producing rate of reactive electron/hole pairs [19–21]. But as a kind of engineering application nanoparticle, the cell cytotoxicity of lanthanide ion doped nano-TiO_2 should be evaluated.

In this paper, Ce (IV) doped TiO_2 nanoparticles (CDTs) were prepared by impregnation method, the cell viability, cell morphology, and cell ultrastructure of L02 cells after exposure to CDTs were examined, and the pathways by which CDTs enter into L02 cells also were investigated.

2. Materials and Methods

2.1. Preparation and Characterization of CDT Nanoparticles. The CDTs were prepared by impregnation technique. A required amount of nanosized anatase TiO_2 was added into milli-Q water, sonication for 15 minutes, then the cerium sulphate [$Ce(SO_4)_2$] aqueous solution was slowly dropped into it under stirring at 60°C for 2 hours; the mixture was filtered, dried at 120°C for 2 hours, and finally calcined at 500°C for 3 hours. The CDTs were characterized by high solution transmission electron microscopy (HRTEM, JEOL JEM 2010, Cs = 0.5 mm, point resolution = 0.19 nm) with a beryllium window energy-dispersive (EDS) detector. The crystallization of CDTs was analyzed by X-ray diffraction (XRD, Rigaku D/max2500).

2.2. Preparation of CDTs Suspension. Firstly, the CDTs were sterilized by autoclaving at 121°C for 30 minutes, then the CDT powder was weighed and resuspended into milli-Q purified water by ultrasonic dispersion method; the suspension was deposited for 30 minutes, then we took the upper of suspension for the next cytotoxicity experiments because of its better dispersibility compared to the lower of suspension. The particle concentration is determined by the following method. After taking away the upper finely dispersed suspension, the weight of CDTs in the remained suspension can be gained through boiling off the water of the suspension, so the weight of CDTs in the finely dispersed suspension can be calculated and the suspension's concentration is also gained. Finally we diluted the gained finely dispersed suspension with Dulbecco's modified Eagle's medium (DMEM, Gibco) for appropriate concentration for the latter using.

2.3. Cell Culture. The Human hepatocyte cell line (L02, provided by State Key Laboratory of Biotherapy, Sichuan university, China) was cultured in DMEM medium containing 10% (v/v) fetal calf serum (FCS), 50 units mL^{-1} penicillin, 50 $\mu g\,mL^{-1}$ streptomycin, and 1% (v/v) 0.2 M L-glutamine at 37°C in a 5% (v/v)of CO_2-humidified atmosphere.

A total of 2×10^5 L02 cells per well were inoculated in 6-wells plates overnight, then medium was replaced with a freshly prepared DMEM/CDTs suspension, with the final concentrations of CDTs 150, 120, 75, and 30 $\mu g\,mL^{-1}$. Culture media without CDT nanoparticles served as the control group in each experiment.

2.4. Cytotoxicity. Cytotoxicity of CDTs on L02 cells was determined by 1-(4,5-dim-ethylthiazol-2-yl)-3,5-diphenylformazan (MTT, Sigma) assay. The cells were seeded in 96-well plates at a density of 1×10^4 cells per well; L02 cells were cultured in the prepared DMEM/CDTs suspension containing different concentrations of CDT nanoparticles for 24, 48, and 72 hours, respectively, then 20 μL of MTT (5 $mg\,mL^{-1}$ in phosphate buffer with pH value equal to 7.4) was added to each well and incubated for 4 hours. Afterward, supernatant was discarded and 50 μL Dimethyl Sulphoxide (DMSO) was added to each well. 15 minutes later, the absorbance of each well was measured at 570 nm with Spectra Max M5 (USA), and the relative cell viability (%) was calculated by the equation [A]test/[A]control × 100%, where [A]test is the absorbance of the treated sample, and [A]control is the absorbance of control sample.

All experiments were repeated 6 times to ensure reproducibility. Experiment data were analyzed by using two-tailed paired *t*-test statistical analysis method.

2.5. Cell Morphology. Cell morphology was investigated by fluorescence microscope and transmission electron microscopy (TEM). For fluorescence microscope observations, after culturing in different media, L02 cells were gently washed with phosphate-buffered saline (PBS) and then fixed in cold ethanol for 15 minutes; after thorough drying; they were stained with Hoechest-33258 (Sigma, 2.5 $mg\,mL^{-1}$) for 5 minutes. Fluorescence microscopic observations were performed by using Olympus BX60 which was equipped with Olympus DP50 digital camera.

For TEM observations, L02 cells were seeded in 75 cm^2 glass culture flask with 10 mL DMEM media for overnight, then the cells were cultured with the DMEM medium containing 150 $\mu g\,mL^{-1}$ concentration of CDTs. In control experiments, medium without CDTs was used. L02 cells were gently washed with PBS and fixed with 0.5%, 3.0% glutaraldehyde in PBS at 4°C for 1 hour, respectively, then postfixed in the media containing 1% osmium tetroxide and 1.5% potassium ferrocyanide for about 1 hour. After thorough washing with PBS, the cells were sequentially dehydrated for 10 minutes each in 50%, 70%, 95%, and 100% ethanol. Finally, the fixed samples were embedded in araldite resin. Serial ultrathin sections (approximately 60 nm in thickness) were gained by ultramicrotome and were stained with uranyl acetate and lead citrate. The

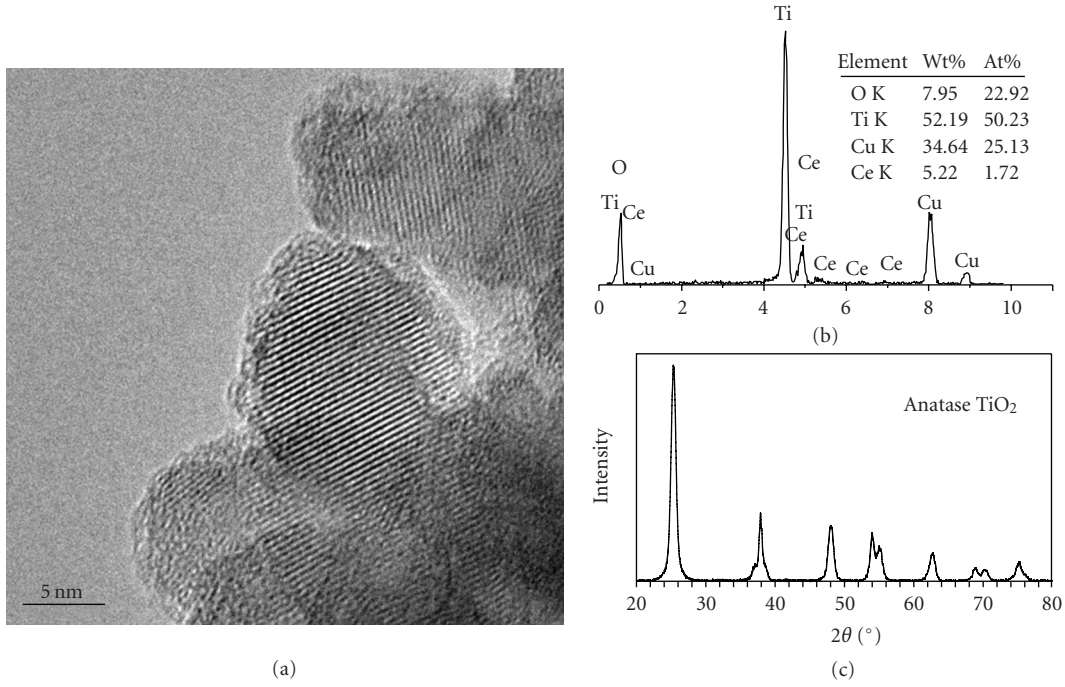

Figure 1: HRTEM image (a), EDS (b), and XRD pattern (c) of CDT nanoparticles.

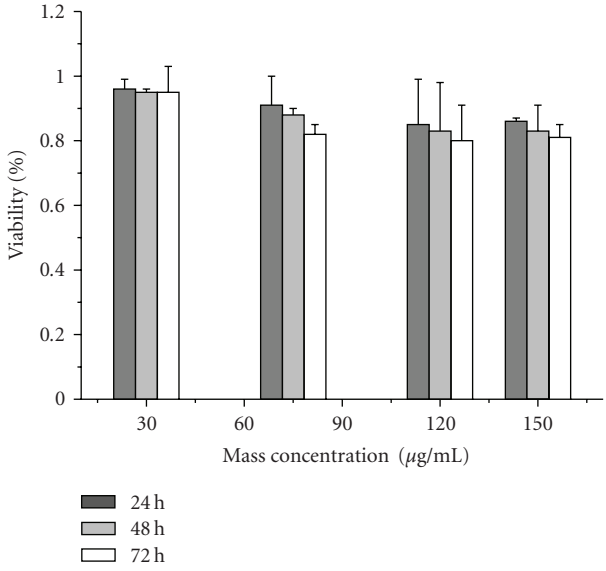

Figure 2: Cell viability of L02 cells exposure to CDT nanoparticles. Cells treated with different concentrations of CDTs for 24, 48, and 72 hours, respectively.

microstructure of cells was examined by TEM (JEOL JEM-1200 EX electron microscope, Tokyo, Japan).

3. Results and Discussions

3.1. Characterization of CDTs. The average particle size of CDTs can be estimated as about 15 nm in the HRTEM measurement (Figure 1(a)). EDS result was shown in Figure 1(b), which indicated that the sample consisted of Ce, Ti, and O elements (Cu element was from the copper grid support). XRD pattern of CDTs in Figure 1(c) showed that the crystalline structure of CDTs was still anatase phase and no rutile TiO_2 or cerium dioxide phase was found, which meant that cerium doping made no change on the anatase structure of original TiO_2 nanoparticles.

3.2. Cytotoxicity of CDTs. The results of MTT assay were shown in Figure 2. The results showed that the cell viability was above 80% when cells were exposed to CDT nanoparticles of different dose from 30 to 150 μg mL^{-1} for 24, 48, and 72 hours, respectively. There is only a slightly decrease in relative growth rate as dose increases from 30 to 120 μg mL^{-1}. The latest investigations [15, 16] strongly supported that nanosized TiO_2 could cause a significant cell viability decrease with UVA irradiation. In our experiments, the cell viability cannot be significantly impaired when L02 cells are exposed to CDT nanoparticles; lack of UV irradiation may be the main reason.

3.3. Morphology and Ultrastructure of L02 Cells. Hoechst 33258 can enter into living cells or dead cells and will emit bright blue fluorescence with UV irradiation. A uniform dispersive blue fluorescence can be found in living cells, whereas, a hyperchromic blocky fluorescence can be observed within the nucleus or cytoplasm of apoptosis cells. Fluorescence micrographs of L02 cells stained with Hoechest 33258 are shown in Figure 3. Cell morphology of treated group and control group was shown in Figures 3(a) and 3(b), respectively, Figures 3(c) and 3(d) were the enlarged view of Figures 3(a) and 3(b), respectively.

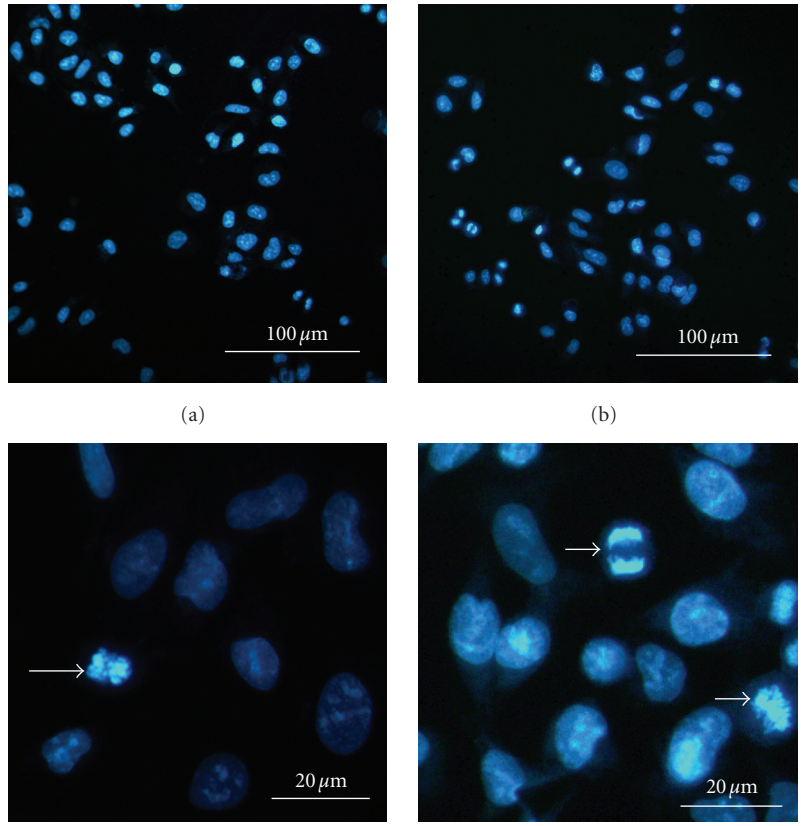

Figure 3: Fluorescence micrographs of L02 cells treated with 150 μg mL^{-1} CDTs for 48 hours. ((a) and (c)) and those of control cells ((b) and (d)). Magnification upper: 400×, lower: 1000×.

Figure 3(a) showed that cells distributed in groups, and the hyperchromic condition of the cells indicated that they were in the S period. Most of the cells exhibited the tight waist shape in the enlarged view (Figure 3(c)), and the cell indicated by arrow in Figure 3(c) was in the middle and later periods of cell division. Figure 3(b) showed that cells in the control group were in normal growing conditions. In Figure 3(d), the cell indicated by the upper arrow was in the later periods of cell division, and the cell indicated by the lower arrow was in the middle periods of cell division. The above analysis showed that, both in treated group and control group, most of the cells appeared with the similar morphology and only the proliferation period was different. Which meant the cell morphology and cell growth could not be obviously influenced when L02 cells were exposed to CDTs; the result is the same as that of MTT assay.

Figure 4 showed the TEM images at different cell division periods of L02 cells exposure to CDT nanoparticles. The cells were in primary, middle and later periods of cell division in Figures 4(a), 4(b), and 4(c), respectively. The normal cell division procedures were observed from Figure 4(a) to Figure 4(c). It seems that there is little influence on the cell division when CDT nanoparticles are in the cell cytoplasm or nucleus.

Ultrastructure of L02 Cells exposed to CDT nanoparticles had shown some differences with that of control cells (Figure 5). The appearance of normal L02 cell is oval shaped and the size is about 12 μm; its ultrastructure was shown in Figure 5(a). The cell nucleus was round with smooth envelope, rough endoplasmic reticulum (RER) and numerous free ribosomes and polysomes were distributed in the cell cytoplasm, meanwhile, round or elongated mitochondria (indicated by the arrows in Figure 5(a)) also scattered in the cytoplasm; distinct cristae could be found in the inner membrane of mitochondria. However, in the ultrastructure of treated cell (Figure 5(b)), some large vacuoles in which there were aggregations of CDTs were found in cytoplasm; some membrane boundaries of these vacuoles became illegible and some membrane boundaries were broken, which led to leaking out of CDT nanoparticles. In addition, it seemed that microstructure of mitochondria was influenced by these CDTs, and the shape of mitochondria (indicated by the arrows in Figure 5(b) was changed, in which the cristae became short or disappeared. Furthermore, In Figure 5(c), it was shown that the smooth envelope around the nucleus was shrank and deformed when the cells were exposed to CDT nanoparticles. Cellular necrosis also was found in treated group (Figure 5(d)).

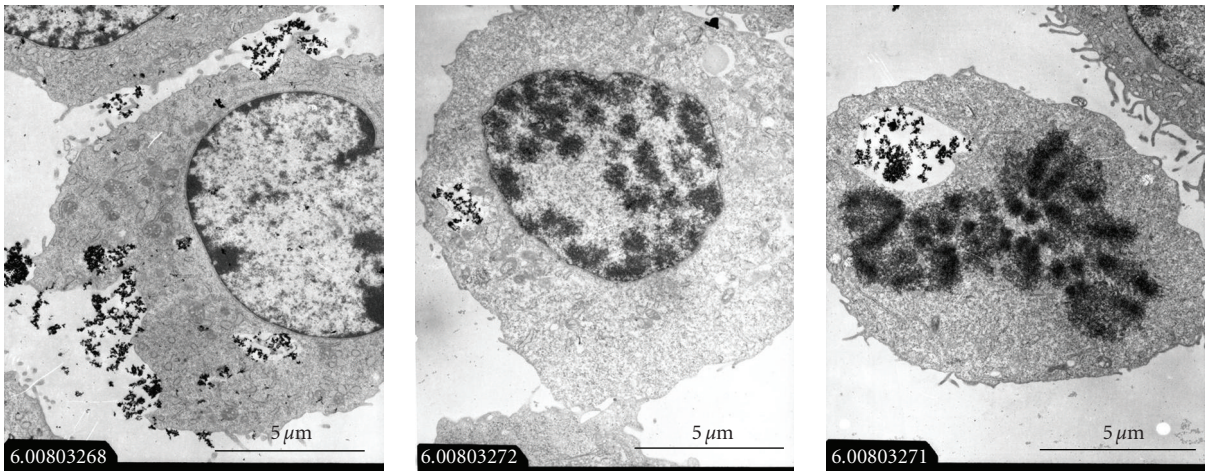

(a) (b) (c)

Figure 4: TEM image of L02 cells treated with 150 mg mL^{-1} CDTs for 48 hours. The cells were at different cell division periods: (a), primary periods, (b), middle periods, and (c), later periods.

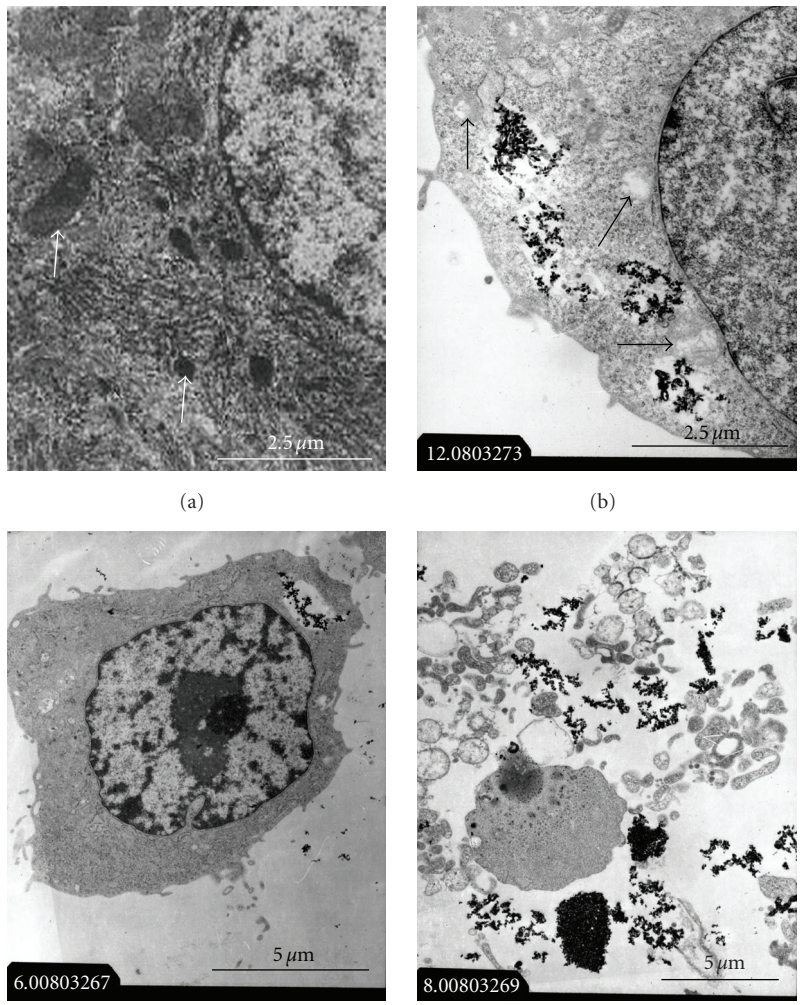

(a) (b)

(c) (d)

Figure 5: Ultrastructure of L02 cells in control group ((a), 12 000×) and in treated group with 150 μg mL^{-1} CDTs for 48 hours ((b), (c), and (d)). Magnification of (b), (c), and (d) is 12 000×, 6 000×, and 8 000×, respectively.

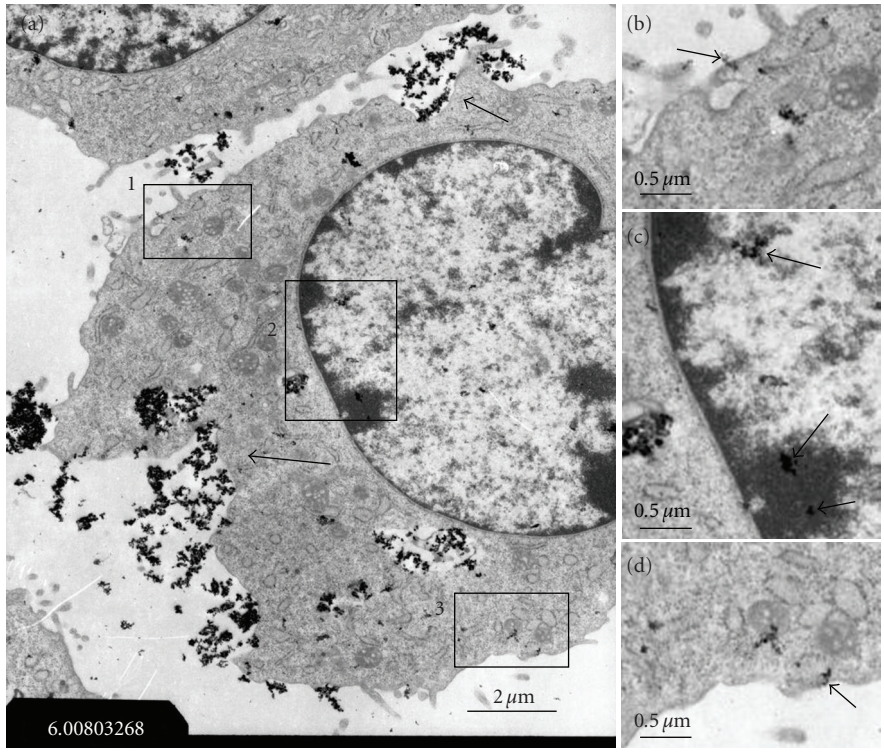

Figure 6: TEM feature of L02 cell after exposure to 150 μg mL^{-1} CDTs for 48 hours. (a) is full view (6,000×). (b), (c) and (d) are the clear magnification of rectangle region 1, 2 and 3 in (a), respectively.

3.4. Uptake Pathway of CDTs in L02 Cells. From the above results of TEM, we found that CDT nanoparticles could enter into L02 cells. It is difficult to gain the living observations of nanoparticles going into cells, so the possible pathways by which CDT nanoparticles went into L02 cells were discussed by analyzing the TEM images.

We found that several CDT nanoparticles could easily gather into a finely ground particle (FGP), and the average size of FGP estimated from the TEM images is about 200 ± 50 nm. And the finely ground particles (FGPs) normally appeared as large aggregations or tiny aggregations in the cells (Figures 4 and 5). We can deduce that these large undispersed nanoparticles got into cells by endocytosis of cell membrane, the regions pointed by the arrows in Figure 6(a) showed that the endocytosis action was happening, and then an endocytic vesicle with membrane-bound was formed in cytoplasm. By the way, these large gathering CDTs were found only in cytoplasm not in nucleus.

Clear magnifications of rectangle regions 1, 2, and 3 were shown in Figures 6(b), 6(c), and 6(d), respectively. Single FGP and tiny aggregations of several FGPs were found in the cell cytoplasm (Figures 6(b) and 6(d)) and nucleus (Figure 6(c), which is indicated by the arrows) without membrane. One part of FGPs in cytoplasm might come from the leakage of nanoparticles from vacuoles, and the other might come from the outside of cells, which suggested that a single CDT or tiny agglomerates of several CDTs can enter into cells by other ways different from endocytosis. We surprisingly found that a tiny aggregation of FGPs pointed by the arrow in Figure 6(b) just inserted in cytoplasm membrane and the cell membrane still kept smooth without deformation. Another tiny aggregation of FGPs indicated by the arrow in Figure 6(d) happened to complete the access procedure. All of these proved that a tiny aggregation of FGPs can directly cross the cell plasma membrane. The way it adopted might be transporting via the channels of substance exchange between the cell and external environment, which was like those for lung-blood substance exchange in the alveolar-airway barrier. The investigations of Conhaim et al. [22] showed that the alveolar-airway barrier consisted not only of tight intercellular junctions that allowed passage of only water and electrolytes but also of a smaller number of large leaks that allowed passage of particles up to nearly 400 nm in radius, maybe similar channel can exist in L02 cells. The shape of tiny aggregation of FGPs pointed by the arrow in Figure 6(b) is like a chain, of which the length is about 220 nm and the width is about 75 nm, so the tiny aggregation of FGPs could carry out the transmembrane action via pores. This kind of passive uptake, not triggered by receptor-ligand interactions, might be activated by electrostatic, Van de Waals, or steric interactions, which were subsumed under "adhesive interactions" by Rimai et al. [23].

The FGPs found in nucleus might be attributed to that the CDT nanoparticle passed through the envelope via the channels provided by nuclear pore complexes (NPCs). Although the channel provided by NPCs is about 9 nm in diameter [24], Panté and Kann reported [25] that ultrafine gold particles coated with cargo-receptor complexes of

up to 39 nm in diameter could pass through the NPCs by signal-mediated transport in xenopus oocytes. In our investigations, the particle size of CDTs is about 15 nm, so it had the ability to pass through the pores. But passing through NPCs needs a signal-mediated mechanism; the mechanism for CDT nanoparticles is not clear and needs further investigation.

In sum, it is very likely that CDT nanoparticles aggregated at cells surface, large aggregations were engulfed by L02 cells by endocytosis and tiny aggregations or even a single nanoparticle could carry out the transmembrane action directly via pores, then a single CDT nanoparticle could enter into nucleus through NPCs channels.

4. Conclusions

(1) Anatase CDTs of mean size about 15 nm were prepared by using impregnating method. Cell viability, cell morphology, cell growth, and cell division periods cannot be influenced when L02 cells are exposed to CDTs of different doses from 30 to 150 μg mL^{-1} without UV irradiation for 24, 48, and 72 hours, respectively. But the ultrastructure of cells has been changed by exposure to CDTs, nucleus was shrank in size and nuclear envelope was deformed, large vacuoles containing CDTs were found in cytoplasm, and the shape of mitochondria was also changed, in which the cristae became short or disappeared.

(2) CDT nanoparticles aggregated at the surface of cells, several CDT nanoparticles easily gathered into a finely ground particle (FGP) with mean size about 200 $\pm$ 50 nm, large aggregations of FGPs entered into L02 cells by endocytosis, and tiny aggregations of FGPs or even a single CDT could cross the cell membrane directly through the channels for mass exchange between the cell and external environment; this action might be activated by adhesive interactions consisting of electrostatic, Van de Waals, or steric interactions, and so forth. Then single CDT nanoparticle could enter into nucleus through nuclear pore complexes (NPCs) channels.

Acknowledgments

This work was supported by National 863 Items of China (no. 2007AA021801, no. 2007AA021901), and the authors thank State Key Laboratory of Biotherapy (Sichuan University, P. R. China) for providing experimental material and apparatus.

References

[1] Y.-M. Kwon, Z. Xia, S. Glyn-Jones, D. Beard, H. S. Gill, and D. W. Murray, "Dose-dependent cytotoxicity of clinically relevant cobalt nanoparticles and ions on macrophages in vitro," *Biomedical Materials*, vol. 4, no. 2, pp. 25018–25052, 2009.

[2] K. Peters, R. E. Unger, C. J. Kirkpatrick, A. M. Gatti, and E. Monari, "Effects of nano-scaled particles on endothelial cell function in vitro: studies on viability, proliferation and inflammation," *Journal of Materials Science: Materials in Medicine*, vol. 15, no. 4, pp. 321–325, 2004.

[3] A. Yamamoto, R. Honma, M. Sumita, and T. Hanawa, "Cytotoxicity evaluation of ceramic particles of different sizes and shapes," *Journal of Biomedical Materials Research*, vol. 68, no. 2, pp. 244–256, 2004.

[4] Q. Zhang, Y. Kusaka, K. Sato, K. Nakakuki, N. Kohyama, and K. Donaldson, "Differences in the extent of inflammation caused by intratracheal exposure to three ultrafine metals: role of free radicals," *Journal of Toxicology and Environmental Health A*, vol. 53, no. 6, pp. 423–438, 1998.

[5] B. Rehn, F. Seiler, S. Rehn, J. Bruch, and M. Maier, "Investigations on the inflammatory and genotoxic lung effects of two types of titanium dioxide: untreated and surface treated," *Toxicology and Applied Pharmacology*, vol. 189, no. 2, pp. 84–95, 2003.

[6] R. Dunford, A. Salinaro, L. Cai, et al., "Chemical oxidation and DNA damage catalysed by inorganic sunscreen ingredients," *FEBS Letters*, vol. 418, no. 1-2, pp. 87–90, 1997.

[7] G. Oberdörster, J. Ferin, R. Gelein, S. C. Soderholm, and J. Finkelstein, "Role of the alveolar macrophage in lung injury: studies with ultrafine particles," in *Environmental Health Perspectives*, vol. 97, pp. 193–199, 1992.

[8] A. L. Di Virgilio, M. Reigosa, and M. F. de Mele, "Response of UMR 106 cells exposed to titanium oxide and aluminum oxide nanoparticles," *Journal of Biomedical Materials Research A*, vol. 92, no. 1, Article ID 19165783, pp. 80–86, 2010.

[9] Q. Rahman, J. Norwood, and G. Hatch, "Evidence that exposure of particulate air pollutants to human and rat alveolar macrophages leads to differential oxidative response," *Biochemical and Biophysical Research Communications*, vol. 240, no. 3, pp. 669–672, 1997.

[10] C.-Y. Jin, B.-S. Zhu, X.-F. Wang, and Q. H. Lu, "Cytotoxicity of titanium dioxide nanoparticles in mouse fibroblast cells," *Chemical Research in Toxicology*, vol. 21, no. 9, pp. 1871–1877, 2008.

[11] Q. Rahman, M. Lohani, E. Dopp, et al., "Evidence that ultrafine titanium dioxide induces micronuclei and apoptosis in syrian hamster embryo fibroblasts," *Environmental Health Perspectives*, vol. 110, no. 8, pp. 797–800, 2002.

[12] J. C. K. Lai, M. B. Lai, S. Jandhyam, et al., "Exposure to titanium dioxide and other metallic oxide nanoparticles induces cytotoxicity on human neural cells and fibroblasts," *International Journal of Nanomedicine*, vol. 3, no. 4, pp. 533–545, 2008.

[13] F. Carinci, S. Volinia, F. Pezzetti, F. Francioso, L. Tosi, and A. Piattelli, "Titanium-cell interaction: analysis of gene expression profiling," *Journal of Biomedical Materials Research B*, vol. 66, no. 1, pp. 341–346, 2003.

[14] J. J. Wang, B. J. S. Sanderson, and H. Wang, "Cyto- and genotoxicity of ultrafine TiO_2 particles in cultured human lymphoblastoid cells," *Mutation Research*, vol. 628, no. 2, pp. 99–106, 2007.

[15] J. F. Reeves, S. J. Davies, N. J. F. Dodd, and A. N. Jha, "Hydroxyl radicals ($\cdot$OH) are associated with titanium dioxide (TiO_2) nanoparticle-induced cytotoxicity and oxidative DNA damage in fish cells," *Mutation Research—Fundamental and Molecular Mechanisms of Mutagenesis*, vol. 640, no. 1-2, pp. 113–122, 2008.

[16] W. F. Vevers and A. N. Jha, "Genotoxic and cytotoxic potential of titanium dioxide (TiO_2) nanoparticles on fish cells in vitro," *Ecotoxicology*, vol. 17, no. 5, pp. 410–420, 2008.

[17] W. Choi, A. Termin, and M. R. Hoffmann, "The role of metal ion dopants in quantum-sized TiO_2): correlation between photoreactivity and charge carrier recombination dynamics,"

Journal of Physical Chemistry, vol. 98, no. 51, pp. 13669–13679, 1994.

[18] U. Diebold, "The surface science of titanium dioxide," *Surface Science Reports*, vol. 48, pp. 53–229, 2003.

[19] M. Anpo and M. Takeuchi, "The design and development of highly reactive titanium oxide photocatalysts operating under visible light irradiation," *Journal of Catalysis*, vol. 216, no. 1-2, pp. 505–516, 2003.

[20] A.-W. Xu, Y. Gao, and H.-Q. Liu, "The preparation, characterization, and their photocatalytic activities of rare-earth-doped TiO_2 nanoparticles," *Journal of Catalysis*, vol. 207, no. 2, pp. 151–157, 2002.

[21] T. H. Hou, J. Mao, X. D. Zhu, and M. J. Tu, "STM and STS investigations of Ce-doped TiO_2 nanoparticles," *Rare Metals*, vol. 25, no. 4, pp. 331–336, 2006.

[22] R. L. Conhaim, A. Eaton, N. C. Staub, and T. D. Heath, "Equivalent pore estimate for the alveolar-airway barrier in isolated dog lung," *Journal of Applied Physiology*, vol. 64, no. 3, pp. 1134–1142, 1988.

[23] D. S. Rimai, D. J. Quesnel, and A. A. Busnaina, "The adhesion of dry particles in the nanometer to micrometer-size range," *Colloids and Surfaces A: Physicochemical and Engineering Aspects*, vol. 165, no. 1–3, pp. 3–10, 2000.

[24] P. L. Paine, L. C. Moore, and S. B. Horowitz, "Nuclear envelope permeability," *Nature*, vol. 254, no. 5496, pp. 109–114, 1975.

[25] N. Panté and M. Kann, "Nuclear pore complex is able to transport macromolecules with diameters of $\sim$39 nm," *Molecular Biology of the Cell*, vol. 13, no. 2, pp. 425–434, 2002.